



Università Degli Studi di Padova

FACOLTA' DI INGEGNERIA

Corso di Laurea in Ingegneria Meccanica

**EFFECT OF SHAFT DIAMETER ON
DARRIEUS WIND TURBINE
PERFORMANCE**

Relatore: Prof. Ernesto Benini

Correlatore: Ing. Marco Raciti Castelli

Laureanda: Micol Chigliaro

Matricola: 459351

ANNO ACCADEMICO: 2012/2013

Index

Index	1
Chapter 1 - Energy Resources.....	3
1.1 Exhaustible Sources	3
1.2 Inexhaustible Sources.....	3
1.3 Renewable Sources	4
Chapter 2 -Wind energy	5
2.1 The wind farm in Italy and Europe	7
2.2 Vertical axis wind turbine	10
2.3 The Savonius turbine.....	11
2.4 The Darrieus Turbine	12
2.5 The micro-wind energy and the urban environment.....	13
Chapter 3 - The wind turbines.....	16
Chapter 4 - Vertical axis wind turbines theory.....	19
4.1 Nomenclature	19
4.2 Hints about the wind	21
4.3 Blades aerodynamic	27
4.4 The Darrieus wind turbine functioning.....	30
Chapter 5 -Effect of Shaft Diameter on Darrieus Wind Turbine Performance.....	32
5.1 Introduction	32
5.2 Model geometry	35
5.3 Discretization of the computational domain	38
5.4 Temporal discretization and Convergence criteria	43
5.5 Results and Discussion.....	44
5.6 Conclusions	48

Nomenclature.....	49
References	50

Chapter 1. - Energy resources

The primary energy sources, that are those directly available in natural environment and by which humanity draws the energy needed for its support and development, are essentially divided in three major groups:

- Exhaustible Sources
- Inexhaustible Sources
- Renewable Sources

1.1 Exhaustible sources

Exhaustible sources include energy resources present in nature in limited quantities and whose regeneration capacity is much lower than the speed of consumption. In this class, you can certainly include fossil fuels, which is exploited in the chemical bonds between the molecules of different species, which belong solid fuels (coal), oil and natural gas.

1.2 Inexhaustible sources.

Although these sources of energy bring into play land reserves over, but the exploitation of the latter would be possible for many thousands of years. This is the case for nuclear energy source, either by fission (new generation reactors) and fusion.

The fast breeder reactors (Superphénix) it would allow the nuclear fission

source for several centuries to ensure the energy needs of the world's consumption.

As for the sources from nuclear fusion, which are still unavailable, due to the current inability to properly control the energy released, the availability of "fuel" would cover the energy needs of humanity for times many orders of magnitude higher than estimated for fission. In the fusion is exploited the binding energy of nuclear nature with phenomena of change and recombination of electrons, neutrons, protons.

1.3 Renewable sources

We define renewable all the sources that regenerate themselves, or those that are restored in a relatively short time in the same quantity in which they are consumed, they are so inexhaustible in a human dimension's time scale. In this large family we may include many types of energy: hydraulic, wind, solar, and ocean wave, ocean thermal gradients, geothermic and biomass.

Chapter 2. - Wind energy.

In the human's history, wind energy has always been an important role for decades to date is a very interesting source of energy for two fundamental reasons:

- the low environmental impact, because there are no emissions into the atmosphere of carbon dioxide and other pollutants;
- its nature, because this source is renewable and inexhaustible.

In the last decade, there has been year-on-year to a remarkable growth of electric wind in the world in terms of installed power, electricity is produced.

Wind power installed globally in 2007 reported a growth of + 25.9% compared to the previous year. At the end of the 2008 annual report of the World Wind Energy Association updates the cumulated world power installed around 121188 MW and wind a percentage equal to 1.5% of the electricity produced and consumed in the world. It is estimated that the wind industry has created until the end of 2008 more than half a million jobs in the world.

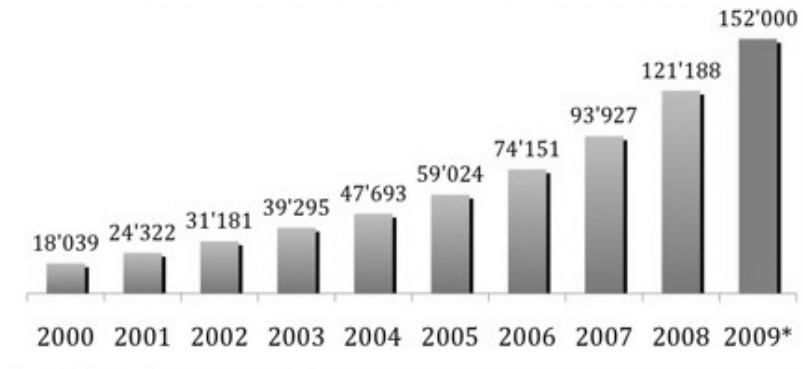


Figure 2.1: MW of total installed wind power capacity worldwide (* indicates a forecast) - source WWEA.

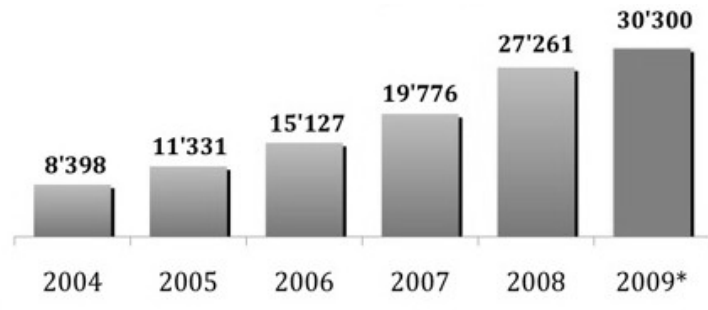


Figure 2.2: New annual installed capacity (in MW) worldwide (* indicates a forecast) - source WWEA

2.1 The wind farm in Italy and Europe

With regard to the old continent, it should be noted that Europe is the leading continent in 2008 to 66160 MW with a total installed power, although its share of annual installed capacity has decreased over the past five years (from 70.7% in 2004 to 32.8% 2008) due to the growth of the wind energy market in the United States and China: the first, in 2008, reached the top spot in terms of total installations, surpassing Germany, while the Chinese market in the same year is shown as one of the most dynamic in the field of wind energy. The European market, even though competition from Asian and American markets, maintains its leadership. The wind energy installed capacity in Europe in 2008 has surpassed all other forms of electricity production: the statistics provided by the European Wind Energy Association show that 36% of all installed capacity in 2008 is made from wind energy.

In Italy, at the end of 2008, the total installed capacity has reached 3736 MW, accounting for 3.1% of the total European Union. Despite the difficulties that the Italian wind farm is located on the side facing the authorization and operating the network connection, the trend of annual installed capacity is positive and increasing in recent years: + 400 MW in 2006, 600 MW in 2007 + and 1000 + MW in 2008. The regions with the most installed wind power are those in the south, where the intensity and frequency of the currents favor a good efficiency of the plants both on land and off-shore.

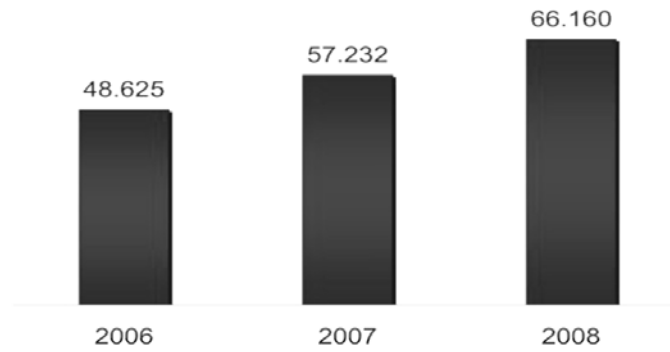


Figure 2.3: Increase in the total wind energy capacity (in MW) installed in Europe, 2006-2008 - source EWEA

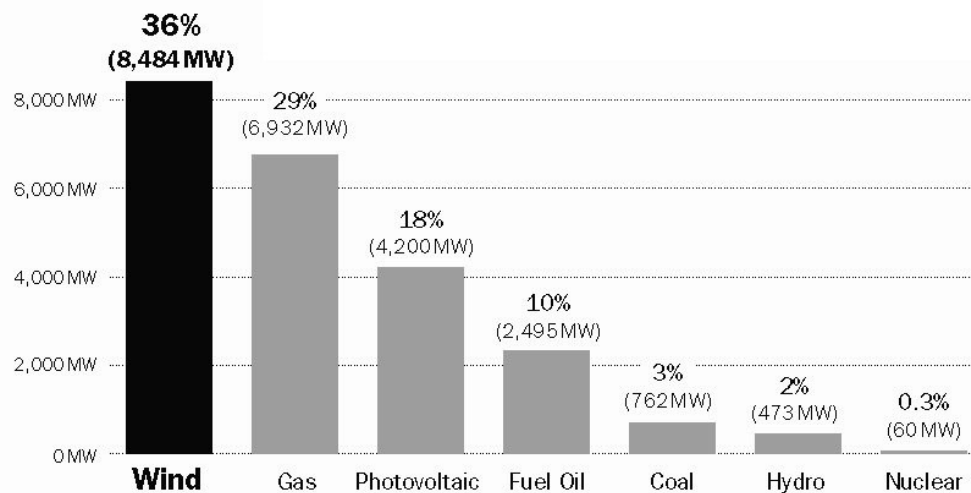


Figure 2.4: New installed capacity in Europe in 2008, differentiated by production technology - source Platts / EWEA

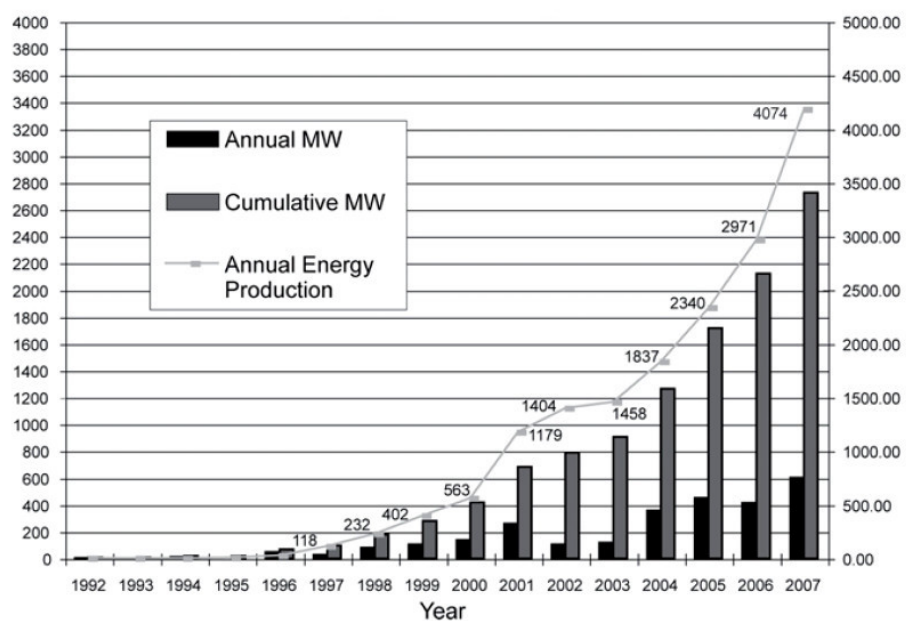


Figure 2.5: Installed capacity (on the left in MW) and annual energy production (right in GWh) in Italy - source: EWEA

2.2 Vertical axis wind turbine.

From the birth of wind technologies, all over the world have been developed and designed machines of various types and shapes. Some of these projects are innovative but not accepted by the commercial point of view. Although there are different ways of classification, in general, we consider two main types of wind turbines: horizontal axis (Horizontal Axis Wind Turbine, in short HAWT) or Vertical Axis (Vertical Axis Wind Turbine, abbreviated VAWT). The first are the most prevalent today, and have the disadvantage of having to be positioned so that the axis is parallel to the wind speed for acceptable performance. The vertical-axis turbines, although less efficiently than the present HAWT, have instead the advantage of operating independently of the wind direction and then to be able to 'pick up' the energy of the wind itself from any direction. The latter class of turbines is divided into two subgroups based on the transmission mechanism of the kinetic energy of the wind: drag driven VAWT (pulse) and lift driven VAWT (aerodynamic).

2.3 The Savonius turbine.

The Savonius turbine was developed by the homonymous Danish engineer in 1931. Its introduction arose much enthusiasm for its structural simplicity: one barrel of oil sold is cut lengthwise in half and the two concavity thus obtained are transferred and fixed on one another to get the power from the two opposing semi-bowl. One of the two concave surfaces receives the current flow and overcoming the resistance to motion of the other surface causes rotation of the machine. For this reason the turbine is also called "a resistance". It is evident that the structure and materials of the rotor are not suitable for high wind speeds. Also it should be noted that the voltage and the output frequency will vary with the wind speed and with the load. This means that this particular turbine cannot be connected directly to the mains, but may find use, for example, in water heating by electrical and in the drive heat pumps, some hydraulic pumps and fans; in such applications in fact prompted a large amount of electricity, so the frequency variations in the operations are not as restrictive as they might seem. The main advantages of this machine are represented by the simple construction, a high strength and a high starting torque, which allows the 'auto start up and operation even in the presence of very weak winds. The operating speed ratios are quite low and generally do not exceed unity. The main disadvantage is the low efficiency that is around 19% - 23% and that restricts the use of the turbine for the production of electricity. The typical fields of application are those where high torques are required at low speeds, such as in pumping water.

2.4 The Darrieus Turbine

Darrieus type turbines are part of the category 'lift driven VAWT'. This model turbine was patented in the United States by aeronautical engineer George French Jean Marie Darrieus, in 1931 . It comprises a number of shaped blades to airfoils, mounted on a rotating shaft which is connected to the electrical generator. There are several variants of design which differ in the shape of the blades. The original design provides for a form to 'blender' named 'troposkein', while other variants are for example with straight blades parallel to the axis of the machine, the so-called 'Giromills', or with the blades wound on a cylindrical surface ideal. There was a real interest for this type of machines until the end of the sixties, when two Canadian researchers from the National Research Council Canada recreated in the same laboratory designed by Darrieus turbine. Then followed several research and experimentation in the United States and Canada, with funding from both public and private. The first commercial VAWT Darrieus was introduced into the market in 1975.

The benefit of these machines lies not only in their simplicity of construction, but especially in the high conversion of efficiency: in fact, the theoretical maximum is 59%, the same wind turbine with a horizontal axis. The high efficiency and high speed ratios make it attractive for the production of electricity. An interesting characteristic is that the rotor produces for each lap a number of peaks of force equal to the number of blades. One disadvantage to point out is the lack of torque that allows the car not starting the machine, so it is necessary to connect an electric motor connected to the network. You can still use an asynchronous machine to solve this problem, because this class of electric machine can operate either as a motor or generator.

2.5 The micro-wind energy and the urban environment

The small size vertical axis turbines are largely used in the field of 'micro-wind', understood as a system of installed capacity and generated order of a few kilowatts (power less than 5 kW). It was above mentioned that the VAWT, unlike horizontal axis wind turbines, operate independently of the flow direction windy and are therefore suitable for an environment characterized by a current that present a high variability in the direction and intensity. This type of conditions are those that occur in an urban environment, which is characterized by a conformation extremely complex and discontinuous, due to the presence of buildings, trees and obstacles of various kinds. Are determined so channeling of currents, winds frequent and sudden changes in flow.

To this is due in recent years the development of micro wind turbines vertical axis in urban and residential, also favored by other important factors: the low noise and visual impact on the territory and positioning at the level of the land or buildings which facilitates maintenance.

The system 'micro-wind' has a great potential: the ability to create a network of distributed generation of electricity that can be stored and consumed on-site, such as residential users or departments. This eliminates the dependence by uncertainty of electricity prices, lowering costs, and making themselves independent, at least in part, from the national grid.

Moreover, this system of distributed micro-generation would significantly reduce energy dependence on fossil fuels. The integration of micro wind energy with other sources, renewable and not, lends itself to be applied in remote areas where there comes the electrical network, such as users at high altitude or on an island.

The period 2007-2008 was a period of great expansion of the global market of mini-and micro-wind, so that there has been a growth of 53% in the first two years. In Italy, the micro wind energy after a first initial development in the early eighties, it was in part abandoned until the following decade, when several private companies have invested in research in this field (you remember the company Tozzi Nord given the collaboration with various universities).



Figure 2.8: Turbina 'Easy Vertical' di Ropatec da 1.0 kW.



Figure 2.9: Turbina 'TN-1,5' prodotta da Tozzi Nord da 1.5 kW.

Chapter 3. - The wind turbines

Wind power is an unlimited and un-polluted energy and it is disposable in many regions of the world. A wind turbine is a fluid dynamic machine able to convert the kinetic energy of an air flow into mechanical energy.

The big world of wind turbines is divided in horizontal axis turbines and vertical axis turbines. Nearly the whole amount of the commercial wind turbines are horizontal axis type (HAWT), with , 3 or 4 pale usually realized in composite material, like carbon fiber and fiberglass, or less frequently, in aluminum. The vertical axis wind turbines (VAWT) are less diffuse, are characterized by a good efficiency with high wind speed, in the state of art, because they use the hydrodynamic lift on the blades to make the airfoils go faster than the flow around the turbine. A Vertical axis wind turbine consists of a number of airfoil vertically mounted on a rotating shaft or a framework.



Figure 3.1: vertical and horizontal axis wind turbines overview

The essential difference between an HAWT and a VAWT is that, during a single rotation of a vertical axis turbine in stationary conditions, the flow direction and wind speed compared to the blades vary recurring in cycles. The power of a turbine, especially of the HAWT, is essentially defined by the rotor diameter. The kinetic energy is transformed in torque on a electric generator functioning following the theory of electromagnetic induction.

The advantages of a VAWT are the following:

- ✓ Simplicity of blade design;
 - ✓ Lack of necessity of over speed control;
 - ✓ Omni-directional operation which is their major strong point, because they use the fluid stream whatever is the flow direction;
 - ✓ Cheapness;
 - ✓ Gearbox and generator can be at one end of the axis;
 - ✓ They do not need pitch and yaw set up and regulations;
 - ✓ Reduction of the mechanical design limitations due to the fact that the control and the electric system are set up statically on the ground.
- One the other hand they have even some great problems, like the impossibility of a self-starting and great loads applied to the blades.

Numerous studies have compared the HAWT and VAWT technologies to determine which is superior. The results are that while the cost of energy for a HAWT may be less than that of a VAWT at a site with high positive wind shear and a prevailing wind direction, the cost of energy for a VAWT may be less at a site with low or negative wind shear or no prevailing wind direction. In addition, there are not enough data available from actual machine operations to answer the question.

One kind of Vertical Axis Wind Turbine is the Darrieus turbine, invented

in 1920 by the Frenchman G. Darrieus and studied in the Seventies. It may have straight blades or curved blades, as shown in the following pictures.

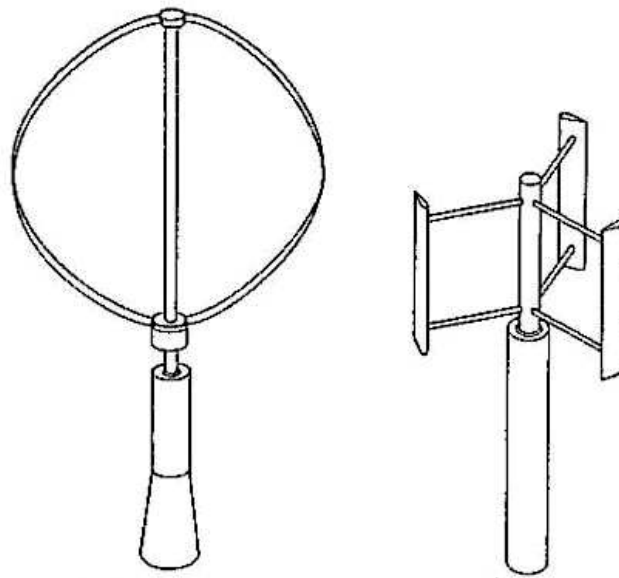


Figure 3.1: curved blade Darrieus wind turbine (a) and straight blade Darrieus wind turbine (b)

Chapter 4. - Vertical axis wind turbines theory

In this chapter there is going to be an analysis of the bases of the wind turbine theory, with a little deepening regarding the vertical axis wind turbine theory.

4.1 Nomenclature

m	mass
ρ	density
ρ_∞	free stream density
v_∞	free stream speed
A_0	area swept by the free stream at the entrance of the turbine
A_p	area swept by the blades
E_c	kinetic energy
E_0	energetic flux di riferimento
C_p	power coefficient
P	power
λ	tip-speed ratio
R	turbine radius
ω	angular velocity
f	frequency
σ	solidity
v_c	cut in speed
v_r	rated wind speed
v_o	cut out wind speed
w	free stream speed on a wing
α	attack angle

c	wing chord
L	lift
D	drag
A_p	airfoil surface
C_L	lift coefficient
C_D	drag coefficient
E	efficiency
R_e	Reynolds number
μ	free stream viscosity
φ	azimuth angle

4.2 Hints about the wind

A wind turbine is a fluid dynamic machine able to convert the kinetic energy of an air flow in mechanical energy. Before describing the vertical axis turbine's physics, it is worth to analyze the dynamic of the wind. [1], [2]

The turbine's skill to produce energy depends on a fundamental parameter: wind speed. The wind speed running over the turbine is higher than the getting out speed, since a part of this kinetic energy is transformed in mechanical energy. Beside this there is an enlargement of the stream lines.

In first analysis it is possible to use the continuity equation:

$$m = \rho_w v_w A_0 = \rho' v' A_f \quad [2.2.1.]$$

and the equation of kinetic energy:

$$E_c = \frac{1}{2} m v_w^2 = \frac{1}{2} \rho_w A_0 v_w^3 \quad [2.2.2.]$$

which explains the energy flux offered by the wind. This flux is not completely used, but there is an important loss: the air mass does not stop passing through the turbine but it has a going out speed, so preserves an amount of kinetic energy which cannot be less of the 40% of the entering one. This statement leads to an important conclusion: in an ideal machine the ideal efficiency of the kinetic-mechanical energy conversion is always less than 60% (Betz limit). It is even compulsory to add the viscous and dissipative losses.

The energetic flux to which engineers refers is:

$$E_0 = \frac{1}{2} \rho_{\infty} A v_{\infty}^3 \quad [2.2.3.]$$

Since this area A is bigger than the entering area A_0 , this energetic flux is bigger than the entering one. The power coefficient is

$$C_p = \frac{P}{E_0} \quad [2.2.4.]$$

where P is the power:

$$P = C_p \frac{1}{2} \rho_{\infty} A v_{\infty}^3 \quad [2.2.5.]$$

Note: it depends on absolute temperature and pressure.

For turbine operating in the subsonic region, the similitude theory is valid. Because of this, tests in the wind tunnels of scaled models are valid if the Reynolds numbers are preserved. This paper is entirely based on this statement, since the tests on the considered vertical axis wind turbine are going to be done in a water basin, keeping the Reynolds number fixed on a scaled model.

Another important equation is the tip-speed ratio or periphery speed ratio:

$$\lambda = \frac{R_{\omega}}{v_{\infty}} = \frac{u}{v_{\infty}} = \frac{\pi D N_r}{60 v_{\infty}}$$

[2.2.6.]

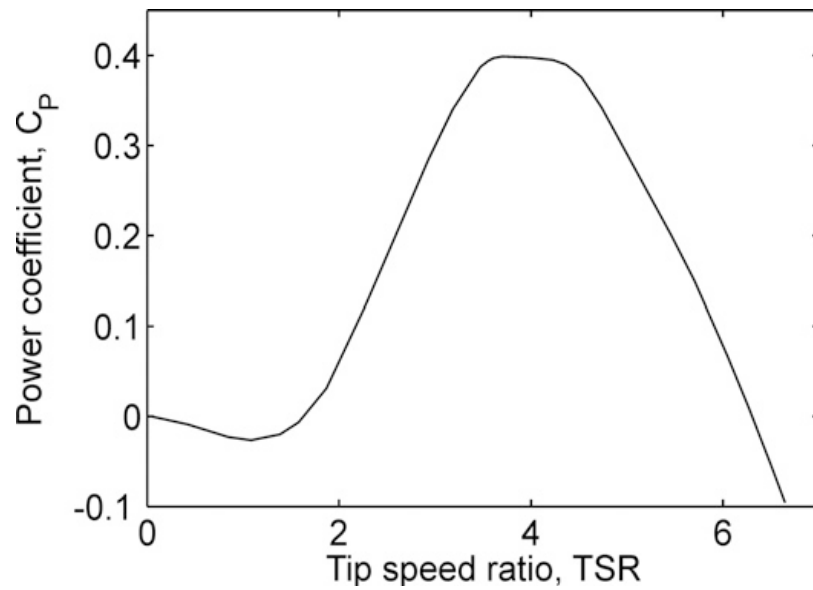


Figure 4.2: trend of a characteristic curve of an VAWT [3].

The power gets higher if the diameter becomes bigger. If the turbine supplies an alternator the frequency is:

$$f = \frac{N_p N_g}{60} \quad [2.2.7.]$$

where N_p is the number of poles couples and N_g is the rpm of the generator.

Finally it is possible to define solidity:

$$\sigma = \frac{A_d}{A} \quad [2.2.8.]$$

where dA is the area occupied by the blades and A is the area of the windblown disc. If solidity gets lower than the space held from the blades in the tube flux gets lower, so the blades speed must be higher to have the same influence on the air flux as a turbine with bigger blades.

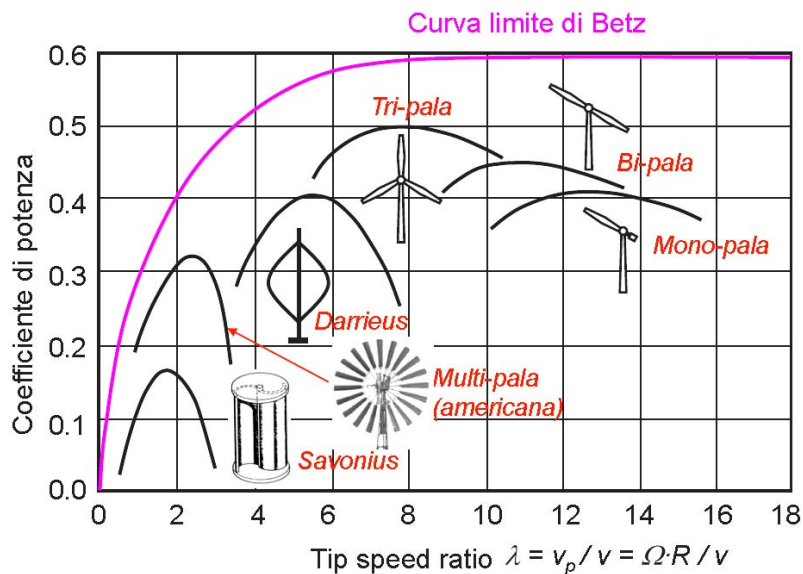


Figure 4.3 : tip speed-solidity curve

The model of a turbine is chosen considering the following characteristics:

- ✓ Cp max;
- ✓ Shape of the tip-speed ratio curve;
- ✓ Solidity.

One of the best compromise is to have low solidity but quite high wind speed. From the equation of power and of the tip speed ratio it is possible to graph the power curves; follows some examples of power curves.

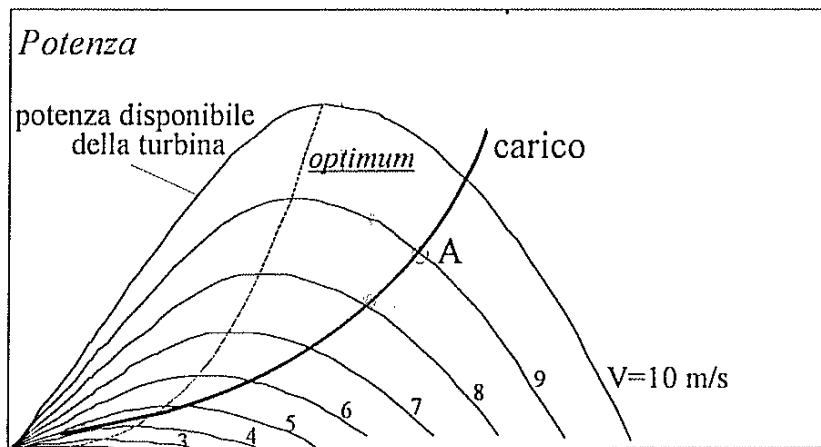


Figure 4.4: power – load curve

Given a wind speed and a diameter it is possible to find out the available power to the turbine shaft. The power output curve for a system constituted of a rotor and generator depends not only on the individual efficiency of both components but also how well they're matched.

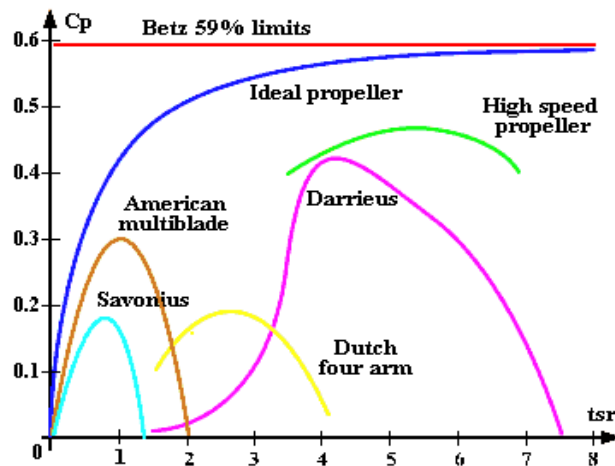


Figure 4.5: Efficiency of a wind turbine plotted in function of C_p and tip-speed ratio. [4]

Finally it is possible to define the following speeds:

- ✓ *cut in wind speed $c v$* : wind speed under which the kinetic energy it is not enough for winning the inner mechanical and electrical resistances. This does not mean that the turbine does not turn but it does not produce power. The cut in speed is usually between 3 and 5 m/s;
- ✓ *rated wind speed $r v$* : wind speed corresponding to the power at full speed;
- ✓ *Cut-out wind speed $o v$* : wind speed which takes the turbine to stop or not to supply power because of safety reason.

4.3 Blades aerodynamic

The blade profile in a wind turbine is determined according to the standard models defined airfoils, which are largely used in the aeronautical field, example in airplane wings, and in the field of turbo machines. The drawing in two dimensions of an aerodynamic profile is obtained overlaying a symmetrical distribution of the thickness to a line average of given shape. The characteristic parameters of a profile are the chord, the maximum thickness s , the lift of the center line by coordinates x_A and y_A . We define also the angles of inclination of the tangents to the edge input θ_i and θ_u to the trailing edge of the medium line, and the angle θ_c formed by these two lines.

The profiles commonly used for a VAWT belonging to the NACA four-digit number, where the first digit indicates the percent ratio y_A / l , the second indicates the ratio x_A / l in tenths, the last two figures give the ratio s in cents. In particular are used symmetrical profiles NACA characterized by a code to four digits, of which the first two are two zeros (that are to indicate the symmetry) and the remaining two percent damage in the relationship between thickness and chord.

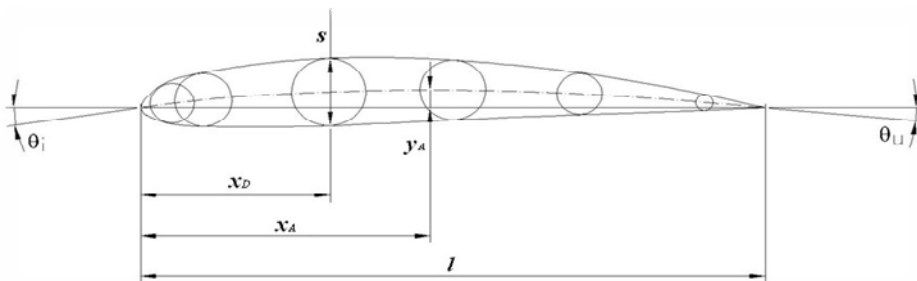
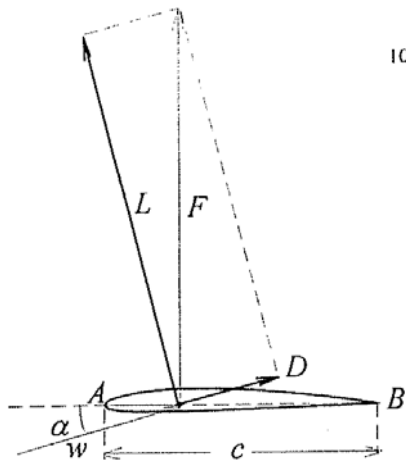


Figure 4.6: Parametri caratteristici di un profilo aerodinamico

Let consider an airfoil put into a free stream with a certain speed w . The angle α between w and the chord c of the airfoil is called attack angle.



NACA 0021

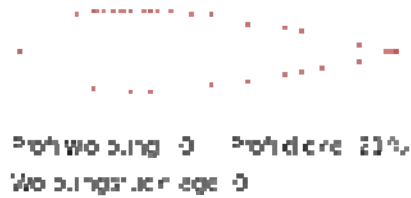


Figure 4.7: forces on an airfoil

The variation of the motion quantity produced by the airfoil into the wind produce a force F on the airfoil which can be broken up into two components: L (lift) and D (drag) which can be state in the following equations:

$$L = C_L \rho \frac{w^2}{2} A_F \quad [2.3.1.]$$

$$D = C_D \rho \frac{w^2}{2} A_F \quad [2.3.2.]$$

$$E = \frac{L}{D} = \frac{C_L}{C_D} \quad [2.3.3.]$$

Where p is the airfoil surface and C_L and C_D are the lift and drag coefficient, depending on the airfoil profile and from the Reynolds number:

$$R_e = \frac{\rho c w}{\mu} \quad [2.3.4.]$$

where μ is the freestream viscosity.

C_L does grow with the growing of the attack angle until this angle does reach a value which correspond with the detach of the fluid from the extrados.

From this moment onward there is a rude decrease of the C_L value while there is a rapid increasing of C_D . This phenomenon is called stall.

4.4 The Darrieus wind turbine functioning.

In this paragraph, the bases of the Darrieus wind turbine functioning theory are going to be explained. To explain the functioning of a Darrieus wind turbine it is possible to consider the following figure:

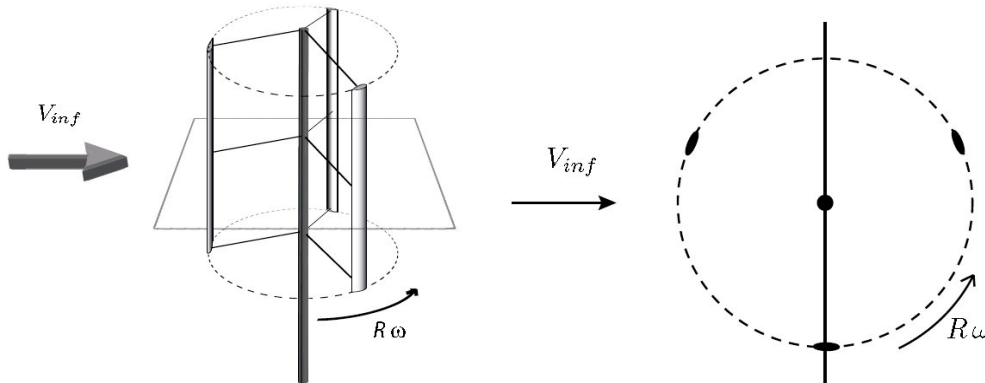


Figure 4.8: functioning scheme of a Darrieus wind turbine

It shows an infinite symmetric wings, rotating with an angular speed ω around an axis with a distance named R . Let's call φ the azimuth angle, which identifies the airfoil position.

As the lift zeroing at the left side (0°) and right side (180°) where the symmetrical airfoil moves paralleled to wind, the torque changes to negative around these position. At the near front (90°) and far back (270°) position, the lift component is much higher than the drag component, so positive torque is produced. The total torque per revolution will be positive with a good set of airfoils so the rotor will accelerate at the right direction.

During the start-up, the starting torque depends on the angular position of rotor with respect to the wind direction, so the rotor might rotate at the right direction straight away or wobble a bit before starting. Normally, the rotor

will need some form of assistance to reach higher rpm before it begins to rotate by itself as the Darrieus rotor has very low torque at low tip-speed ratio, which can be easily worsened (till negative) by friction in the system.

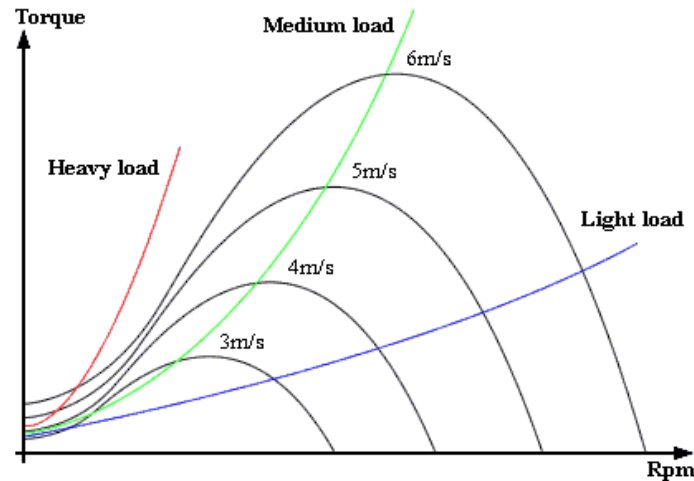


Figure 4.9: torque –speed plot

The plot above shows a torque of a rotor at different wind speed. The colored curves are the load/torque that is required to turn the generator at different rpm. A light load will cause the rotor to operate at very high rpm (high tip speed ratio) which will not maximize the rotor efficiency while the heavy load causes the rotor to rotate slowly (low tip speed ratio) which also do not maximize the rotor efficiency. By selecting a load nearer to the rotor maximum efficiency point like the medium curve, more power can be obtained. The peak torque may not be the peak power and for the case of Darrieus rotor, the peak power normally occurs after the peak torque. Another Darrieus rotor behavior is the low starting torque which might be lower than the resisting generator torque, so the rotor will not start unless given some push until certain rpm where the rotor torque starts to overcome the load torque. [4]

Chapter 5. - Effect of Shaft Diameter on Darrieus Wind Turbine Performance

5.1 Introduction

A growing interest is registered as far as the use of wind turbines inside urban areas is concerned. Due to the unpredictability and unsteadiness of the airflow close to buildings, conventional horizontal-axis wind turbine (HAWT) designs result in a low efficiency, because of their requirement to be set into the wind direction in order to operate at maximum efficiency. Thanks to its inherent capability of operating independently from the incoming wind direction, an effective alternative to HAWTs is represented by the vertical-axis design, which has now reached first-generation production level. Moreover, vertical-axis wind turbine (VAWT) maximum power coefficient can be obtained at lower tip-speed ratio if compared with conventional HAWTs, thus reducing flow induced noise. However, little is known about such turbine noise generation. Hence, as observed by Sezer-Uzol et al. (Sezer-Uzol et al., 2009), the accurate predictions of aerodynamic loads and noise become a challenging key issue in the design process of wind turbines, in consideration of their intended locations. As pointed out by Pedersen (Pedersen, 2007), on the one hand, there is a social requirement for erecting more wind turbines in order to generate electricity without harm to the environment; on the other hand, there is an individual need for quiet and peace in the home environment: both these demands have to be met in the future developments of wind turbine design.

The influence of the central shaft on the overall noise emission of a straight-bladed vertical-axis Darrieus wind turbine was investigated by Raciti Castelli and Benini (Raciti Castelli and Benini, 2011). A simplified aeroacoustic model, based on the analysis of pressure fluctuations at discrete and fixed rotor azimuthal positions along the blade trajectory was proposed, allowing a correlation between rotor dynamic characteristics, such as torque and power coefficients, and acoustic measurements. The results of two-dimensional simulations were proposed for a classical NACA 0021 three-bladed rotor operating at optimum tip speed ratio: a sharp correspondence was registered between the azimuthal positions of maximum power generation and the ones of maximum noise emission, once again confirming wind turbine noise emission to be strictly connected with power generation. A dramatic influence of the central shaft was also registered, causing marked oscillations in the measured acoustic values, due to the passage of the downwind blade into the wake generated from the rotor shaft itself and causing a low frequency pulsation whose period is connected to rotor angular velocity.

The aim of the present work is to investigate the effect of the shaft dimension on the aerodynamic performance of a straight-bladed Darrieus VAWT of 1.03 m diameter. For such purpose, four rotor architectures are compared: a no-shaft configuration and three configurations characterized by shaft diameters of 50 mm, 100 mm and 300 mm. The numerical set up is based on the CFD simulations already presented by Raciti Castelli et al. (Raciti Castelli et al., 2011). The non-linear governing equations for the conservation of mass, momentum and turbulence are solved sequentially (i.e., segregated from one another) by the proprietary code Ansys Fluent 13.0, which is based on a finite volume method. The complete validation of

the present numerical simulations is based on the wind tunnel measurements illustrated in (Raciti Castelli et al., 2010) and is not reported here again for brevity's sake.

5.2 Model geometry.

The hereby numerical analyses are based on the Darrieus wind turbine already analyzed by (Raciti Castelli et al., 2010), whose main features are summarized in Table 1. The solidity is defined as:

$$\sigma = Nc/R_{\text{rotor}} \quad [5.3.1]$$

as suggested by Strickland (Strickland, 1975).

Figure 1 shows the adopted reference system for the definition of the rotor location during its revolution: the azimuthal position is identified by the angular coordinate of the pressure centre of blade No. 1 (set at $0.25c$ for the NACA 0021 airfoil), starting between the 2nd and the 3rd Cartesian plane octants.

Table 1:

Main features of the tested rotor configurations

<i>Parameter</i>	<i>Value</i>
$D_{rotor} [mm]$	1030
$H_{rotor} [mm]$	1 (2D simulation)
$D_{shaft} [mm]$	50; 100; 300
$N [-]$	3
$c [mm]$	85.8
$\sigma [-]$	0.5
$A [mm^2]$	1030
$\omega [rad/s]$	from 25.1 to 57.6
$\rho [kg/m^3]$	1.225
$V [m/s]$	9

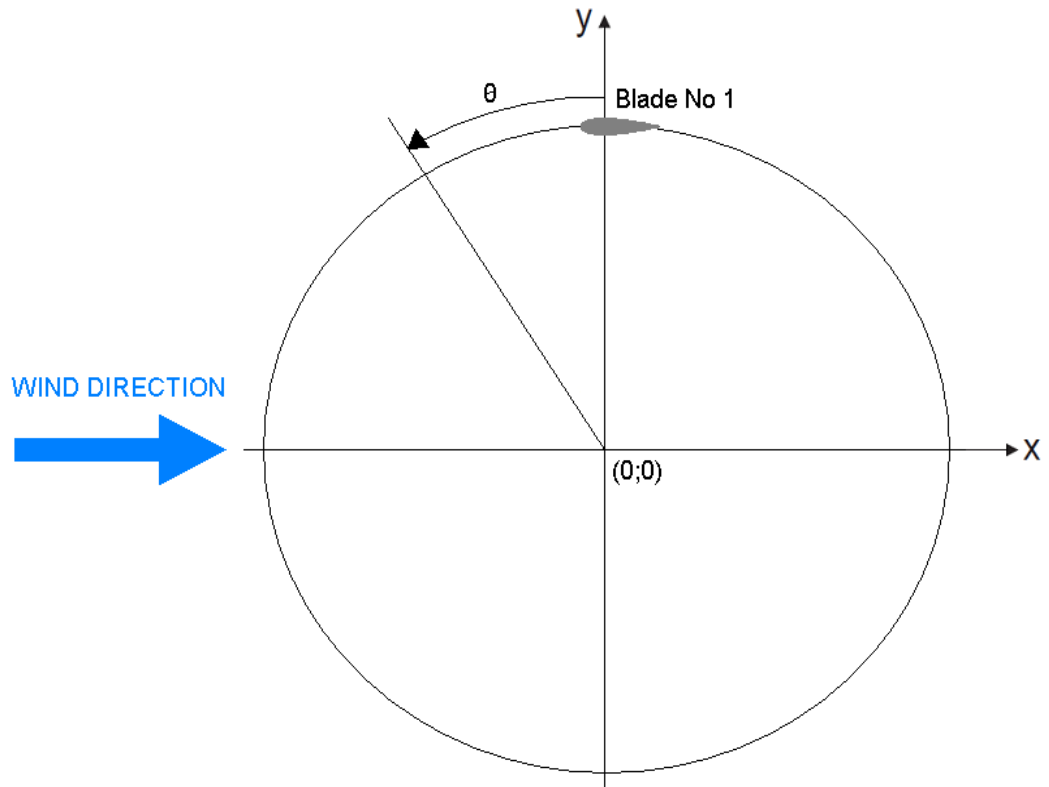


Figure 5.1: Azimuthal coordinate of blade No. 1 centre of pressure

5.3 Discretization of the computational domain.

The 2D computational domain is herein discretized by two grids: a fixed outer one and a rotating inner one. The use of a moving sub-grid is mandatory, due to the movement of the rotor blades. In order to allow a full development of the wake, Simao Ferreira et al. (Simao Ferreira et al., 2007) placed inlet and outlet boundary conditions respectively 10 rotor diameters upwind and 14 rotor diameters downwind with respect to the rotor test section for a CFD simulation of a rotor operating in a wind tunnel. As the aim of the present work is the simulation of a turbine operating in open field conditions and because of the huge domain width necessary to avoid solid blockage, inlet and outlet boundary conditions are hereby placed 37 rotor diameters upwind and 60 rotor diameters downwind with respect to the rotor test section. Figure 2 shows the main dimensions and the boundary conditions of the computational domain. As can be seen, the overall computational domain width results nearly 80 rotor diameters, in order to avoid the effect of wake blockage on the unperturbed free-stream velocity, as suggested from (Raciti Castelli et al., 2011).

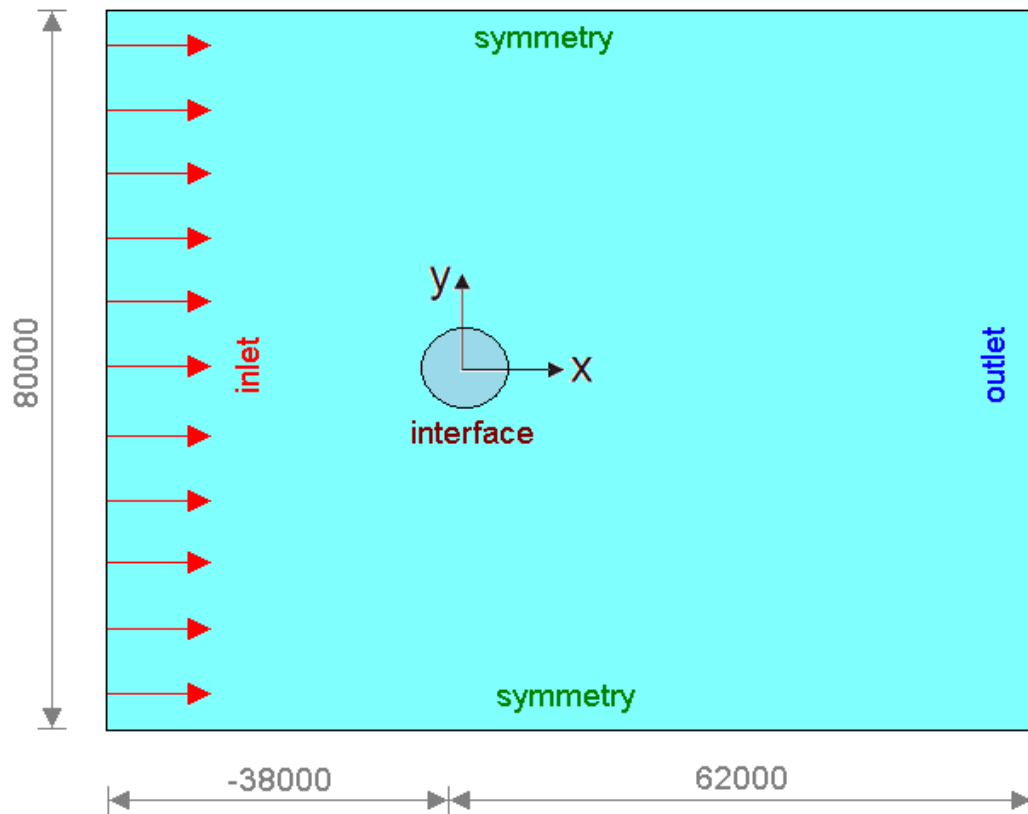


Figure 5.2: Main dimensions [mm] and boundary conditions of the computational domain (the darkest area represents the rotational domain, where both rotor blades and the shaft are modeled).

Two *Symmetry* boundary conditions are imposed at the two side walls. The circumference around the circular opening centered on the turbine rotational axis is set as an *Interface*, thus ensuring the continuity in the flow field. An unstructured mesh is chosen for both fixed and rotating grids, in order to reduce engineering time to prepare the CFD simulations. The rotating sub-grid is the fluid area simulating the revolution of the wind turbine and is therefore characterized by a moving mesh, rotating at the same angular velocity of the turbine. Its location coincides exactly with the circular opening inside the fixed sub-grid area and is centered on the turbine rotational axis.

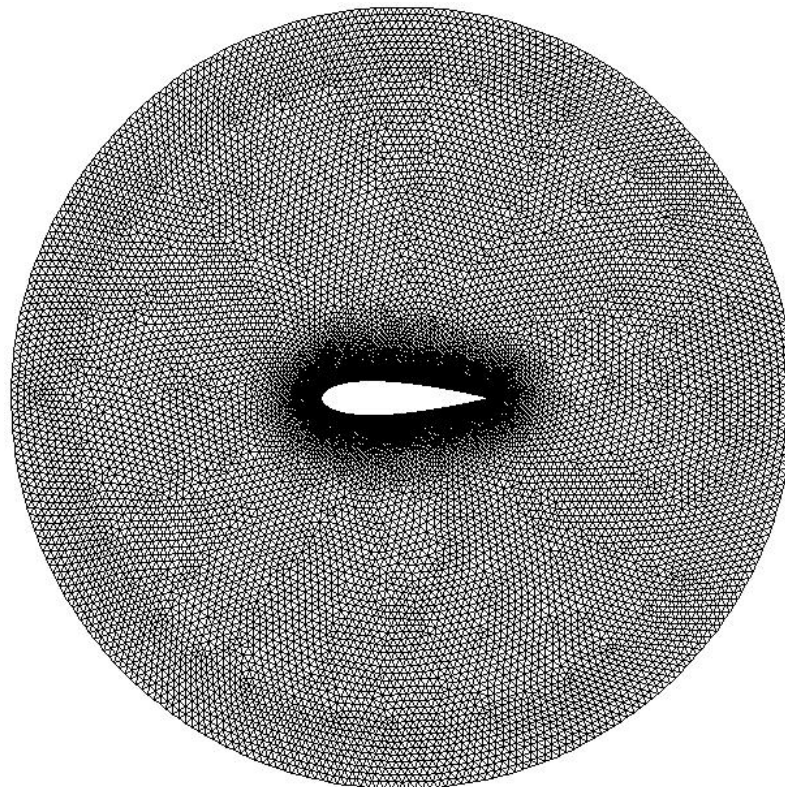


Figure 5.3: Near blade mesh for the NACA 0021 blade section.

Table 2:

Main geometrical features of the near-blade mesh

<i>Description</i>	<i>Value</i>
<i>Number of grid points on airfoil upper/lower surface [-]</i>	3600
<i>Minimum grid point spacing (on airfoil leading edge) [mm]</i>	0.015
<i>Maximum grid point spacing (on airfoil trailing edge) [mm]</i>	0.025
<i>Growth factor from airfoil leading edge to airfoil trailing edge [-]</i>	1.005
<i>Growth factor from airfoil surface to rotating sub-grid area [-]</i>	1.1

All blade profiles inside the rotating sub-grid area are enclosed in a control circle of 400 mm diameter. Unlike the *Interface*, it has no physical significance: its aim is to allow a precise dimensional control of the grid elements in the area close to rotor blades by adopting a first size function operating from the blade profile to the control circle itself and a second size function operating from the control circle to the whole rotating sub-grid area, ending with grid elements of the same size of the corresponding fixed sub-grid elements. An *Interior* boundary condition is used for control circle borders, thus ensuring the continuity of the cells on both sides of the mesh. Some details of the grid are visible in Figure 3, while Table 2 summarizes the main geometrical features of the near-blade mesh: grid independent solutions are found using an unstructured mesh topology with approximately 10^6 cells. For more information about mesh generation and code validation, see also (Raciti Castelli et al., 2011).

5.4 Temporal discretization and Convergence criteria.

The adopted commercial CFD package is Ansys Fluent 13.0, which implements 2D RANS equations using a finite volume based solver. The fluid is assumed to be incompressible, being the maximum fluid velocity in the order of 60 m/s. The temporal discretization is achieved by imposing a physical time step equal to the lapse of time the rotor takes to make a 1° rotation. As a global convergence criterion, each simulation is run until instantaneous torque coefficient values show a deviation of less than 1% compared with the corresponding values of the previous period, corresponding to a rotation of 120° due to rotor three-bladed geometry. Residual convergence criterion for each physical time step is set to 10^{-5} . The present simulations require about 16 CPU seconds per physical time step. An average of about 30 sub-iterations is necessary to converge the solution at each physical time step. The simulations, performed on an 8 processor, 2.33 GHz clock frequency computer, have required a total CPU time of about 10 days each.

5.5 Results and Discussion.

Figure 4 shows the evolution of the power coefficient, defined as:

$$C_p = P / (\frac{1}{2} \rho A V^3) \quad [5.5.1]$$

as a function of the tip speed ratio, defined as:

$$\lambda = \omega R_{\text{rotor}} / V \quad [5.5.2]$$

While vanishing differences are registered between the no-shaft configuration and the one characterized by a shaft diameter of 50 mm, some differences are visible for the rotor configuration characterized by a shaft diameter of 100 mm. The marked detrimental effect of the rotor configuration characterized by a shaft diameter of 300 mm is clearly visible. It can also be observed that the position of maximum rotor efficiency ($\lambda \sim 2.4$) is roughly constant.

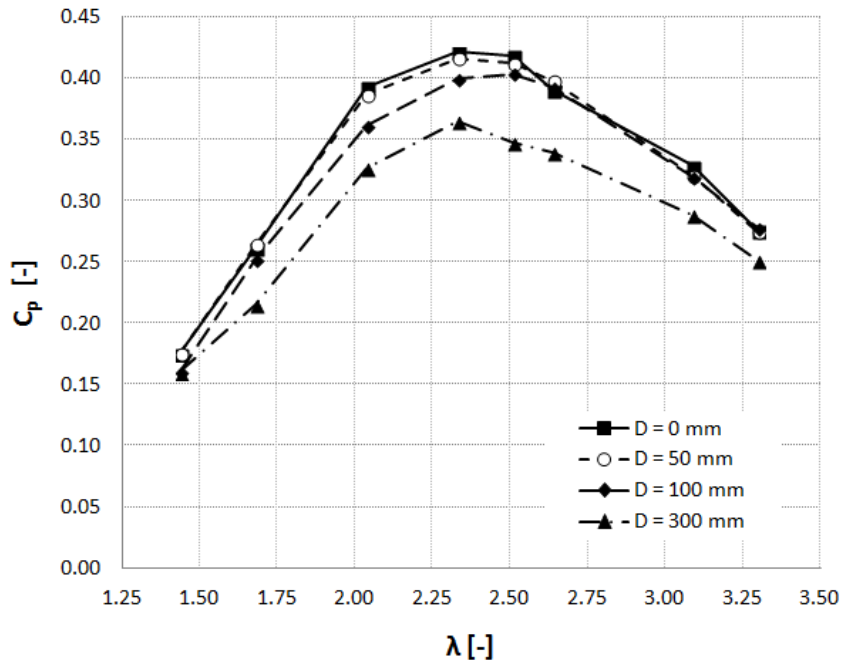


Figure 5.4: Evolution of rotor power coefficient as a function of the tip speed ratio

The reduction of overall rotor performance with the increment of its shaft diameter can be ascribed to the corresponding reduction of the wind speed inside the rotor disk (especially in the downwind portion of blade revolution, due to the wake of the shaft), as can be clearly seen from Figures 4, 5, 6 and 7, showing the contours of the absolute velocity for the four tested rotor architectures at $\theta \sim 90^\circ$, corresponding to the azimuthal position of maximum power production, as observed by (Raciti Castelli et al., 2011).

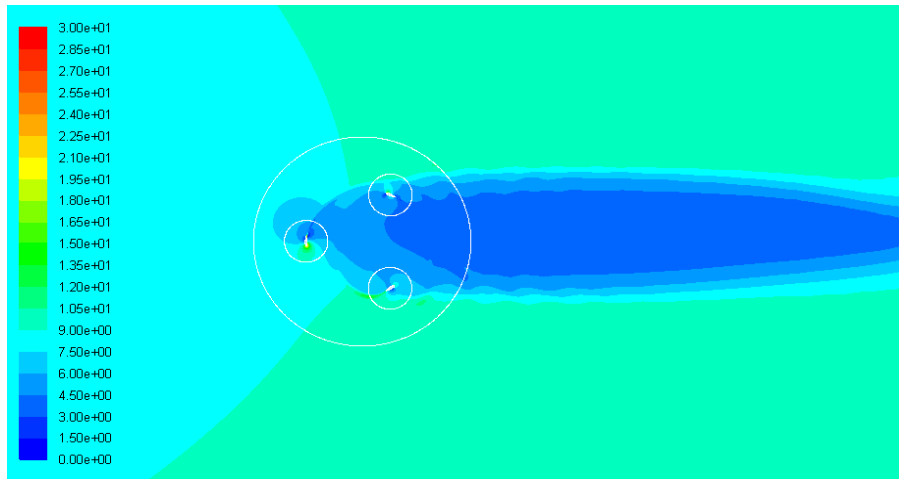


Figure 5.5: Contours of absolute velocity [m/s] for the no-shaft rotor configuration; $\lambda=2.33$, $\theta=90^\circ$

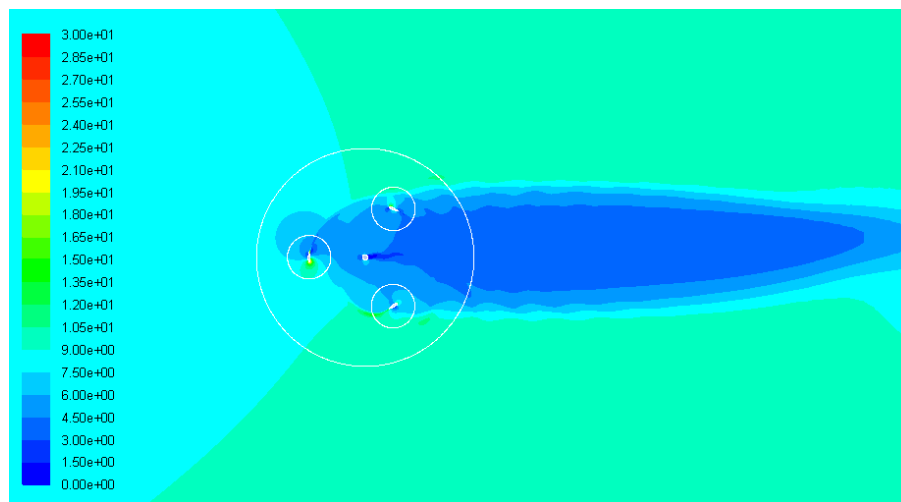


Figure 5.6: Contours of absolute velocity [m/s] for the rotor configuration characterized by a shaft of 50 mm diameter; $\lambda=2.33$, $\theta=90^\circ$

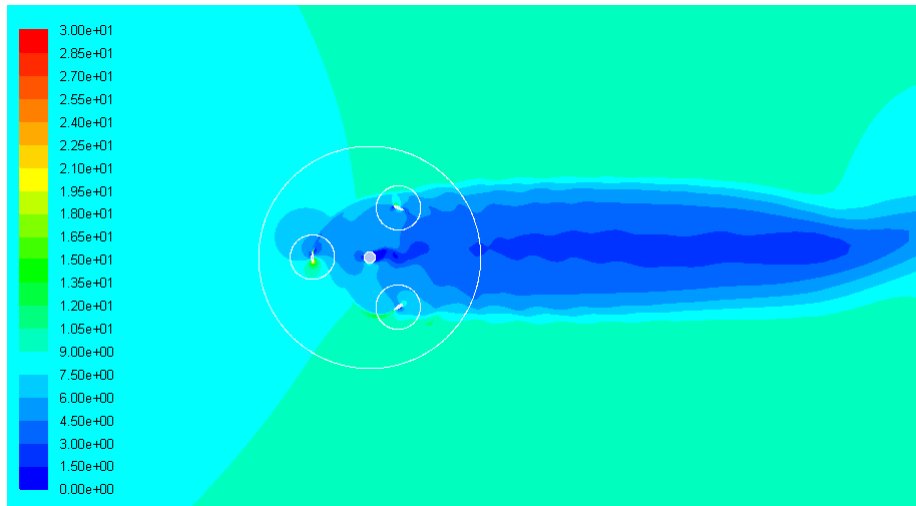


Figure 5.7: Contours of absolute velocity [m/s] for the rotor configuration characterized by a shaft of 100 mm diameter; $\lambda=2.33$, $\theta=90^\circ$

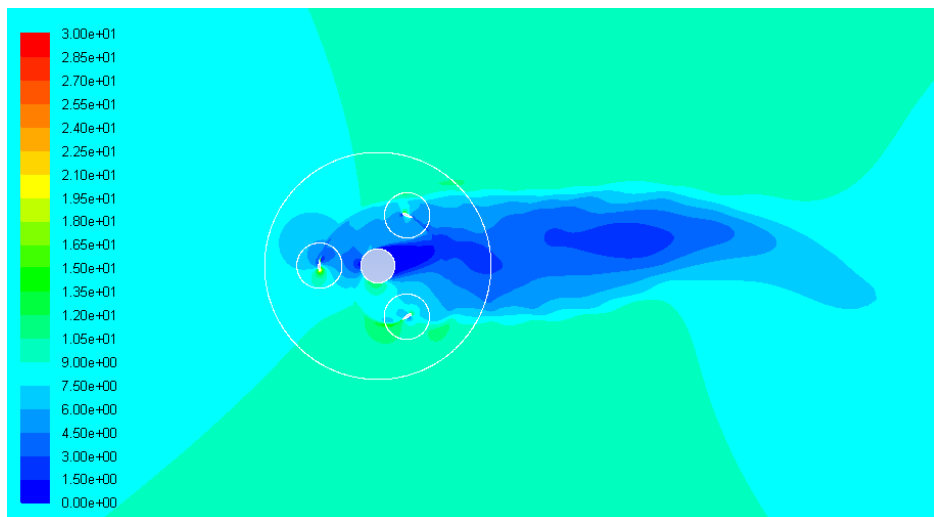


Figure 5.8: Contours of absolute velocity [m/s] for the rotor configuration characterized by a shaft of 300 mm diameter; $\lambda=2.33$, $\theta=90$

5.6 Conclusions.

The influence of the central shaft on the aerodynamic performance of a straight-bladed Darrieus vertical-axis wind turbine has been investigated by means of a full campaign of numerical simulations on a three-bladed rotor configuration of 1.03 m diameter. Both a no-shaft architecture and some configurations characterized by different shaft diameters (50 mm, 100 mm and 300 mm) have been investigated.

A marked reduction of overall rotor performance with the increment of its shaft diameter has been registered. Such decrease in rotor aerodynamic efficiency is to be ascribed to a reduction of the wind speed inside the rotor disk, especially in the downwind portion of the blade revolution, due to the wake of the shaft. It has also been observed that the azimuthal position of maximum rotor efficiency is not influenced by the shaft diameter.

Nomenclature.

A [mm^2]	rotor swept area
c [mm]	blade chord
C_p [-]	rotor power coefficient
D_{rotor} [mm]	rotor diameter
D_{shaft} [mm]	shaft diameter
H_{rotor} [mm]	rotor height
N [-]	rotor blade number
P [W]	rotor aerodynamic power
R_{rotor} [mm]	rotor radius
V [m/s]	unperturbed wind velocity
θ [$^\circ$]	blade azimuthal position
λ [-]	rotor tip speed ratio
ρ [kg/m^3]	air density
σ [-]	rotor solidity
ω [rpm]	rotor angular velocity

References.

Pedersen, E. (2007) *Human Response to Wind Turbine Noise – Perception, Annoyance and Moderating Factors*, Doctoral Thesis, Goteborg Universitet.

Raciti Castelli, M., Benini, E. (2011) *CFD Analysis of the Influence of Central Shaft on Vertical-Axis Wind Turbine Noise Emission*, Fourth International Meeting on Wind Turbine Noise, Rome, Italy, 12-14 April, 2011.

Raciti Castelli, M., Ardizzon, G., Battisti, L., Benini, E., Pavesi, G. (2010) *Modeling Strategy and Numerical Validation for a Darrieus Vertical Axis Micro-Wind Turbine*, ASME 2010 International Mechanical Engineering Congress & Exposition, Vancouver (British Columbia), November 12-18, 2010, IMECE2010-39548.

Raciti Castelli, M., Englaro, A., Benini, E. (2011) *The Darrieus wind turbine: Proposal for a new performance prediction model based on CFD*, Energy, Vol. 36, No. 8, pp. 4919-4934.

Sezer-Uzol, N., Gupta, A., Long, L. N. (2009) *3-D Time-Accurate Inviscid and Viscous CFD simulations of Wind Turbine Rotor Flow Fields*, Lecture Notes in Computational Science and Engineering, Vol. 67, pp. 457-464.

Simao Ferreira, C. J., Bijl, H., van Bussel, G., van Kuik, G. (2007) *Simulating Dynamic Stall in a 2D VAWT: Modeling Strategy, Verification*

and Validation with Particle Image Velocimetry Data, The Science of Making Torque from Wind, Journal of Physics: Conference Series 75.

Strickland, J. H. (1975) *The Darrieus Turbine: A Performance Prediction Model Using Multiple Streamtube*, SAND75-0431.